

# ASSESSING LANDFILLS SURFACE TEMPERATURE DISTRIBUTION USING LANDSAT 8 SATELLITE IMAGE AT BIG CITIES IN VIETNAM

Trinh Le Hung<sup>1,\*</sup>, Tong Thi Hanh<sup>1</sup>

<sup>1</sup>Le Quy Don Technical University

## Abstract

In recent years, rapid urbanization and population growth have led to an overload of waste in big cities. High landfill surface temperature is an important factor causing serious environmental pollution due to speeding up the generation of biogas. This paper presents the results of assessment of land surface temperature distribution in some large landfills in Vietnam, including Nam Son landfill (Hanoi) and Da Phuoc landfill (Ho Chi Minh city). Landsat 8 satellite image data is used to calculate land surface temperatures based on the split-window method. The results showed that the landfill surface temperature was much higher than the surrounding area, even compared to the areas characterized by impervious surfaces. The difference between the highest surface temperature in Nam Son, Da Phuoc landfills and the lowest surface temperature in the surrounding area is about 20°C. The results obtained in this study provide input information to develop monitoring models of pollution at landfills.

**Keywords:** Landfill; land surface temperature; remote sensing; thermal infrared; Landsat 8.

## 1. Introduction

Urbanization is an inevitable development trend of all countries in the world, especially for developing countries like Vietnam. Rapid urbanization and population growth have led to an overload of waste in big cities, causing serious environmental pollution, especially in the area around landfills. The process of decomposing organic substances in landfill generates biogas such as carbonic (CO<sub>2</sub>), methane (CH<sub>4</sub>), ammonia (NH<sub>3</sub>), hydrogen sulfide (H<sub>2</sub>S). High land surface temperature is also an important factor causing more serious pollution in landfill due to speeding up the generation of biogas. The use of remote sensing data to determine the landfill surface temperature is a practical application, providing information to help managers in dealing with environmental pollution in the area around the landfills.

Since the last of 20<sup>th</sup> century, remote sensing technique has had many advantages in comparison to the more traditional methods and can be effectively used for land

---

\* Email: [trinhlehung@lqdtu.edu.vn](mailto:trinhlehung@lqdtu.edu.vn)

surface temperature monitoring (Bui, 2015 [2]; Tran et al., 2009 [19]). The main data in determining land surface temperature is thermal infrared imagery, such as Landsat, Aster and MODIS. These studies show that the difference between the land surface temperature calculated from remote sensing data and the temperature at field measurement stations usually does not exceed 1.5 degrees (Tran et al., 2009 [19]; Trinh and Vu, 2019 [21]). The applications of thermal infrared remote sensing data include urban heat island phenomenon monitoring, subsurface coal fires mapping and drought study. Several recent studies have used Landsat thermal infrared data to assess landfill surface temperature distribution (Qdais and Shatnawi, 2019 [14]; Gills et al., 2019 [8]; Dancheva et al., 2019 [5]). These studies have shown that the landfill surface temperature is often significantly higher than the surrounding area temperature.

A number of algorithms have been used to estimate the land surface temperature using remote sensing thermal infrared (TIR) data as it is capable to decipher the thermal characteristic of the land surface. These algorithms are namely mono-window, split-window, dual-angle, single-channel... (Galve et al., 2008 [7]; Rongali et al., 2018 [15]). Single-channel algorithms to estimate land surface temperature from one thermal band have advantage over other methods when the imageries with only one thermal band are used, such as Landsat TM, Landsat ETM+ data (Chen et al., 2015) [4]. Meanwhile, the split-window method is more effectively used for remote sensing data with multiple thermal infrared bands (Yu et al., 2014 [22]).

Landsat 8 is the eighth satellite in the Landsat program, which provides images at 11 spectral channels, including 2 thermal infrared bands at a spatial resolution of 100 m (band 10 (10.60-11.19  $\mu\text{m}$ ) and band 11 (11.50-12.21  $\mu\text{m}$ )) [25]. Until now, most studies have used only band 10 of Landsat 8 image to calculate land surface temperature (Boori et al., 2015 [1]; Guha et al., 2018 [9]; Pal and Ziaul, 2017 [13]; Trinh, 2018 [20]). A number of studies have used the split-window method to calculate land surface temperature based on using both Landsat 8 infrared thermal bands (Yu et al., 2014 [22]; Li and Jiang, 2018 [12]). The studies carried out in different areas, such as the northern Negev Desert, Israel (Du et al., 2014 [6]; Rozenstein et al., 2014 [17]), the Beas River basin, India (Rongali et al., 2018 [15]) and Binh Phuoc province, Vietnam (Trinh and Vu, 2019 [21]) show that the split-window algorithm can be adjusted for estimating land surface temperature from Landsat 8 data to get better accuracy.

The objective of this paper is to assess the distribution of land surface temperature in Nam Son landfill (Ha Noi) and Da Phuoc landfill (Ho Chi Minh city) using Landsat 8

data. These are the two largest landfills in Vietnam and are suffering from overload and serious pollution. Split-window algorithm was used to calculate land surface temperature from Landsat 8 data in this case study. In this study, image processing is done by using ERDAS Imagine 2014 program, and landfill surface temperature maps were created using ArcGIS 10 program. From brightness temperature and land surface emissivity images, the landfill surface temperature image was obtained by using Spatial Modeler tool of ERDAS Imagine 2014 program.

## 2. Materials and Methodology

### 2.1. Materials

In this study, two multispectral cloud-free LANDSAT 8 OLI\_TIRS images with a spatial resolution of 30 meters of multispectral bands and 100 meters of thermal infrared bands acquired from September 30, 2019 and January 6, 2020 (Figure 1) were used to calculate surface temperature at landfills. The LANDSAT 8 data was the standard terrain correction products (L1T), downloaded from United States Geological Survey (USGS – <https://earthexplorer.usgs.gov/>) website [26].

The Landsat 8 satellite was launched by NASA on February 11, 2013, and operates in a sun-synchronous orbit with a 16 day repeat cycle. The Landsat 8 OLI\_TIRS sensors acquires 11 spectral bands along a 185 km orbital split-window ath [25]. Characteristics of Landsat 8 satellite bands are shown in Table 1.

Table 1. Characteristic of Landsat 8 satellite imagery

Band	Name	Wavelength (µm)	Spatial resolution (m)
1	Coastal/Aerosol	0.433 – 0.453	30
2	Blue	0.450 – 0.515	30
3	Green	0.525 – 0.600	30
4	Red	0.630 – 0.680	30
5	Near Infrared	0.845 – 0.885	30
6	Sortware infrared	1.560 – 1.660	30
7	Sortware infrared	2.100 – 2.300	30
8	Panchromatic	0.500 – 0.680	15
9	Cloud/Cirrus	1.360 – 1.390	30
10	Thermal infrared	10.30 – 11.30	100
11	Thermal infrared	11.50 – 12.50	100

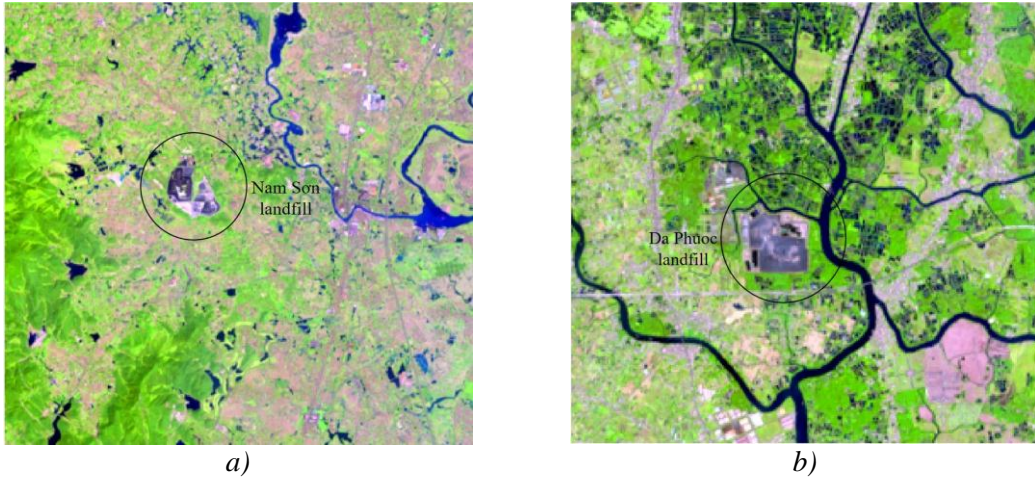


Figure 1. Landsat 8 satellite images in Nam Son landfill (a) and Da Phuoc landfill (b)

## 2.2. Methodology

The split-window algorithm is based on the different atmospheric absorption behavior of two radiometric channels within the 10-12.5 $\mu\text{m}$  window region (Rongali et al., 2018 [15]). The basis of the split-window algorithm is the radiance attenuation for atmospheric absorption, which is proportional to the radiance difference of simultaneous measurements at two different wavelengths, each of them being subject to varying amounts of atmospheric absorption (Rongali et al., 2018 [15]). According to this algorithm, land surface temperature can be determined by the following formula (Jiménez-Muñoz et al., 2014 [11]):

$$T_s = T_{B10} + c_1(T_{B10} - T_{B11}) + c_2(T_{B10} - T_{B11})^2 + c_0 + (c_3 + c_4W)(1 - \varepsilon) + (c_5 + c_6W)\Delta\varepsilon \quad (1)$$

where  $T_s$  is land surface temperature;  $T_{B10}$ ,  $T_{B11}$  are brightness temperatures of band 10 and 11 of Landsat 8 imagery;  $W$  is atmospheric water vapor content ( $\text{g}/\text{cm}^2$ ). The value of atmospheric water vapor content is calculated using formula proposed by Huazhong (Huazhong et al., 2014 [10]);  $\varepsilon$  is mean emissivity;  $\Delta\varepsilon$  is emissivity difference;  $c_0$  to  $c_6$  are split-window coefficients values. The values of split-window coefficients are given in Table 2 (Sobrino et al., 2006 [18]).

Table 2. Split-window coefficient values for TIRS band of Landsat 8 imagery [18]

No.	Constants	Value
1	$c_0$	-0.268
2	$c_1$	1.378
3	$c_2$	0.183
4	$c_3$	54.300
5	$c_4$	-2.238
6	$c_5$	-129.200
7	$c_6$	16.400

The flowchart of split-window algorithm utilized in the present study for the estimation of land surface temperature is shown in Figure 2.

In first step, OLI and TIRS band data must be converted to TOA spectral radiance using the radiance rescaling factors provided in the metadata file:

$$L_{\lambda} = M_L \cdot Q_{cal} + A_L \tag{2}$$

where  $L_{\lambda}$  is TOA spectral radiance (Watts/(m<sup>2</sup>.srad.μm));  $M_L$  is band-specific multiplicative rescaling factor from the metadata (RADIANCE\_MULT\_BAND\_x, where x is the band number);  $A_L$  is band-specific additive rescaling factor from the metadata (RADIANCE\_ADD\_BAND\_x, where x is the band number);  $Q_{cal}$  is quantized and calibrated standard product pixel values (DN).

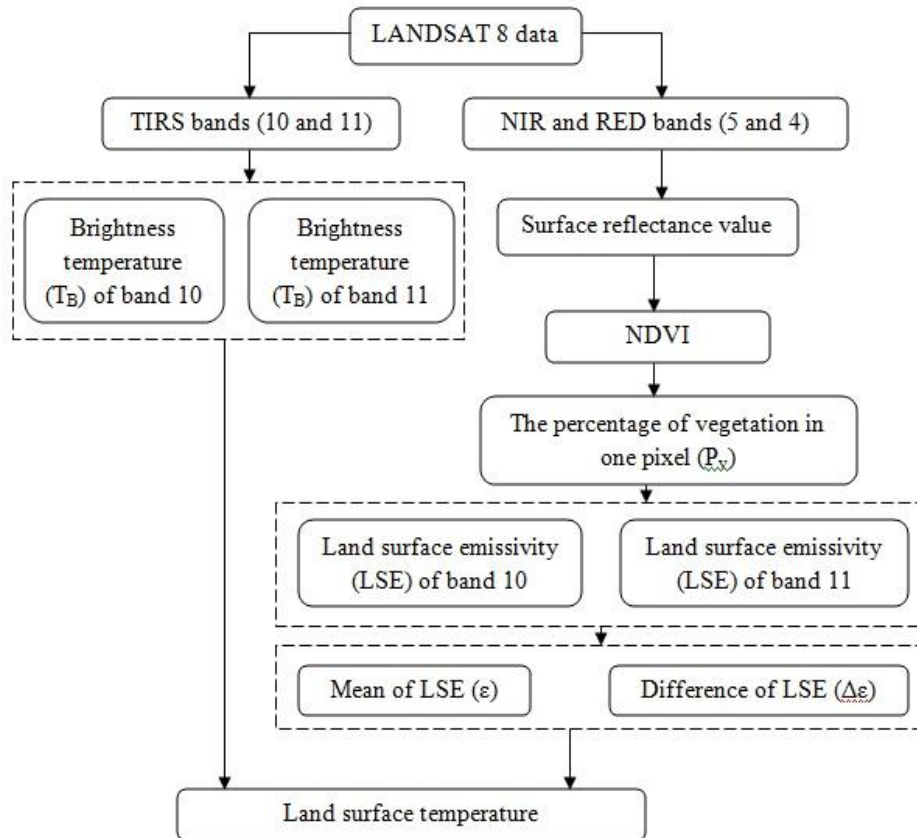


Figure 2. Split-window algorithm for land surface temperature retrieval

Table 3. Landsat 8 TIRS spectral radiance  $M_L$ ,  $A_L$  dynamic ranges [25]

No.	Data type	Band	$M_L$	$A_L$
1	Landsat 8 TIRS	10	$3.342 \cdot 10^{-4}$	0.1
2	Landsat 8 TIRS	11	$3.342 \cdot 10^{-4}$	0.1

In second step, the Landsat 8 thermal band data (band 10 and band 11) can be converted from spectral radiance to brightness temperature using following equation:

$$T_B = \frac{K_2}{\ln\left(\frac{K_1}{L_\lambda} + 1\right)}, \quad (3)$$

where  $T_B$  is at satellite brightness temperature (K);  $K_1$  is calibration constant 1 ( $W/(m^2 \cdot sr \cdot \mu m)$ );  $K_2$  is calibration constant 2 (K).

Table 4. Landsat 8 thermal band calibration constants [25]

No.	Data type	Band	$K_1$ ( $W/(m^2 \cdot sr \cdot \mu m)$ )	$K_2$ (Kelvin)
1	LANDSAT 8	10	774.89	1321.08
2	LANDSAT 8	11	480.89	1201.14

For determining land surface temperature from Landsat 8 data, values of land surface emissivity are needed. In this paper, the surface emissivity is determined by using method based on NDVI image, which proposed by Valor and Caselles (1996) [23] by following equation:

$$\varepsilon = \varepsilon_v \cdot P_v + \varepsilon_s (1 - P_v) \quad (5)$$

where  $\varepsilon$  is surface emissivity;  $\varepsilon_v$ ,  $\varepsilon_s$  are emissivity of pure vegetation covers and pure soil areas, respectively;  $P_v$  is the percentage of vegetation in one pixel, which calculated by equation (Vlassova et al., 2014 [24]):

$$P_v = \left( \frac{NDVI - NDVI_{soil}}{NDVI_{veg.} - NDVI_{soil}} \right)^2 \quad (6)$$

where  $NDVI$  is normalized difference vegetation index, which can be calculated by equation (Rouse et al., 1973 [16]):

$$NDVI = \frac{NIR - RED}{NIR + RED} \quad (7)$$

$RED$  and  $NIR$  are the spectral reflectance in red and near-infrared band, respectively;  $NDVI_{veg.}$  and  $NDVI_{soil}$  are the  $NDVI$  values of vegetation and open soil, which are determined experimentally using a series of test area for vegetation and open soil.

For calculating  $NDVI$  index, the digital number of red and near infrared band was converted to surface reflectance value. In this study, one very advanced atmospheric approach (FLAASH) has been applied on the Landsat 8 multispectral image, and then, the  $NDVI$  is calculated according to Equation (7).

The land surface emissivity images of bands 10 and 11 are used to calculate mean and difference emissivity:

$$\varepsilon = \frac{\varepsilon_{10} + \varepsilon_{11}}{2}, \quad (8)$$

$$\Delta\varepsilon = \varepsilon_{10} - \varepsilon_{11} \quad (9)$$

In last step, land surface temperature can be calculated by equation (1).

### 3. Result and Discussion

#### *Test area No.1*

Nam Son landfill - located in Soc Son district, is the largest landfill in Hanoi, which was put into operation in 1999. It is the main waste treatment area of four urban districts of Hanoi with about 4000 tons/day. Nam Son landfill has an area of about 83 ha, with 9 standard waste areas. In recent years, the environmental pollution in the area around Nam Son landfill has been serious, greatly affecting the lives of people.

Landsat 8 satellite images taken on September 30, 2019 (path/row 127/045) were used to calculate surface temperature. The thermal infrared bands (band 10 and band 11) were used to calculate brightness temperature; the red (band 4) and near infrared band (band 5) were used to calculate surface emissivity based on normalized difference vegetation index (NDVI). From brightness temperature and land surface emissivity images, the land surface temperature image was obtained by using Spatial Modeler of ERDAS Imagine 2014 program. Figure 3 shows the spatial distribution of land surface temperature around Nam Son landfill, which obtained from Landsat 8 satellite image. The land surface temperature in test area No.1 ranged from 24.1 to 45.9°C, in which, high land surface temperatures are concentrated locally in Nam Son landfill area. The landfill surface temperature is much higher than the surrounding area, even compared to the residential and construction land, which characterized by impervious surfaces.

In Figure 3, eight zones are identified with the following temperatures: less than 30°C, 30-32°C, 32-34°C, 34-36°C, 36-38°C, 38-39°C, 39-40°C and greater 40°C. It can be seen, the landfill surface temperature is higher than 40°C (shown in red color). Nam Son landfill surface temperature is also much higher than average land surface temperature (about 32°C).

Figure 4 shows a cross-section of land surface temperature at the Nam Son landfill. As can be noticed, the landfill surface temperature has increased dramatically compared to the surrounding area. Most of the surrounding area has temperatures lower than 35°C, while landfill temperatures are higher than 43°C, even higher than 45°C. The land

surface temperature of the waste storage area is also significantly higher than other areas in the landfill, as shown by the concave position of the graph in Figure 4.

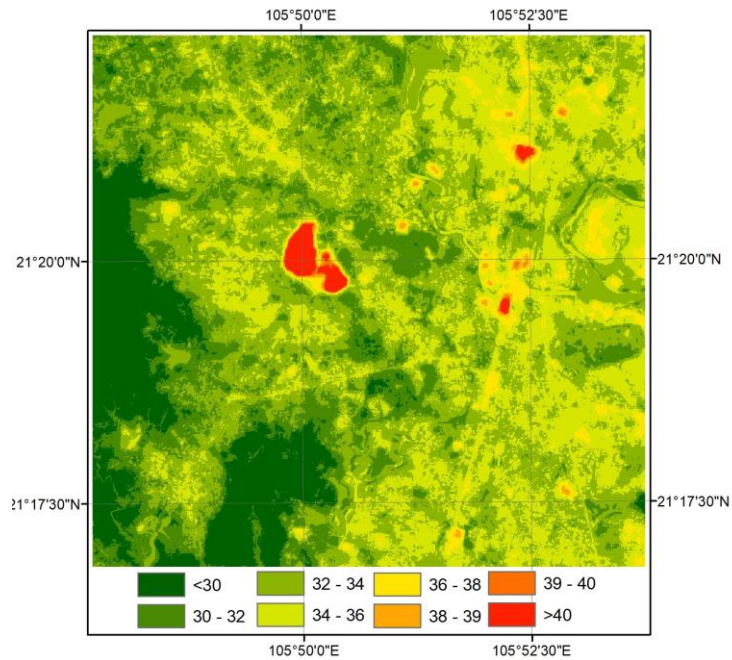


Figure 3. Land surface temperature distribution map of Nam Son landfill

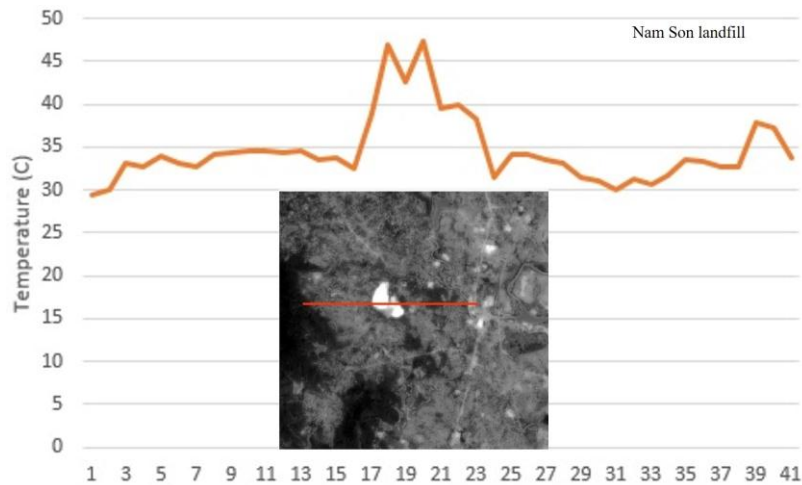


Figure 4. Cross section of land surface temperature at the Nam Son landfill

**Test area No.2**

Da Phuoc Waste Treatment Complex is located in Da Phuoc commune, Binh Chanh district, Ho Chi Minh city (southern Vietnam). It has a total area of 600 ha, in which the core area is arranged landfill of about 300 ha. The amount of waste processed daily in Da Phuoc reaches about 50000 tons.

Landsat 8 satellite images taken on January 6, 2020 (path/row 125/052) were used to calculate land surface temperature. The land surface temperature distribution map in Da Phuoc landfill and surrounding area is presented in Figure 4. The results showed that the distribution of land surface temperature in the test area No.2 in January 6, 2020 ranged from 25.5-45.7°C, the average temperature is 30.3°C. Similar to Nam Son landfill, the surface temperature of the Da Phuoc landfill is much higher than the surrounding area and the average land surface temperature (about 32°C). Most of Da Phuoc landfill area has surface temperature over 40°C, about 20°C higher than the area covered by vegetation. As with test area No.1, in Figure 4, eight zones are identified with the following temperatures: less than 28°C, 28-30°C, 30-32°C, 32-34°C, 34-36°C, 36-38°C, 38-40°C and greater 40°C. It is noticeable that the Da Phuoc landfill surface temperature (shown in red color) is clearly differentiated from surrounding areas, even compared to Long Hau urban areas in the south of the study area (shown in range color).

Figure 6 shows a cross-section of land surface temperature at the Da Phuoc landfill. Similar to Nam Son landfill, the cross section of surface temperature at Da Phuoc landfill also showed a sudden increase compared to the surrounding area. The temperature difference at the edge of the landfill and the center of the landfill reaches the highest of about 20 degrees.

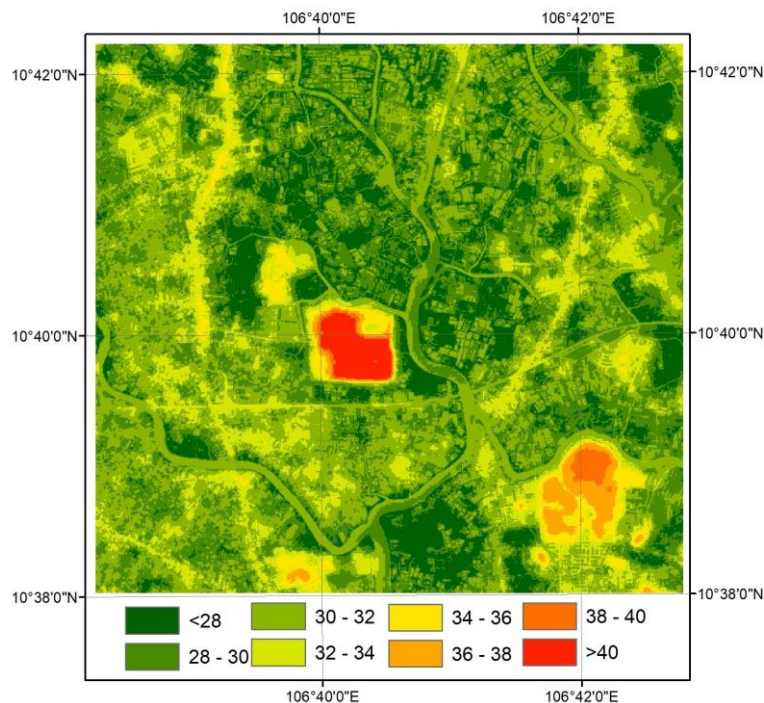


*Figure 5. Land surface temperature distribution map of Da Phuoc landfill*

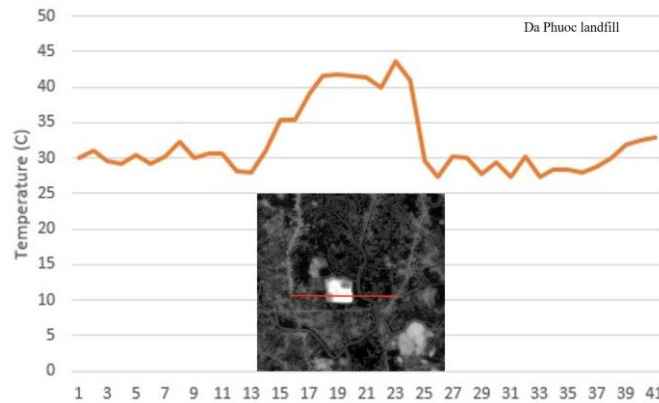


Figure 6. Cross section of land surface temperature at the Da Phuoc landfill

### Accuracy assessment

Due to the long distance between the two experimental areas (over 2000 km), in this study we only measured land surface temperature in the area around Nam Son landfill (Hanoi city) by thermometer. Measurement data at 10 sample points (Fig. 7) at 10 a.m. September 30, 2019 was used to compare with temperature values retrieval from Landsat 8 image, which acquired from same day. Figure 8 presents some pictures in the survey in the study area, including incinerators, garbage dump and wastewater treatment facilities.

Comparison between land surface temperature values retrieved from Landsat 8 image and measurement data is presented in Table 5. Analysis of the results obtained in Table 5 shows that, at 10 sample points, the land surface temperature retrieved from the Landsat 8 satellite image is higher than the measurement temperature. Despite of that, the difference between them is not high, about 2.5 degree on average.



Figure 7. Location of the land surface temperature measurement points

Table 5. Comparison between land surface temperature values retrieved from Landsat 8 data (September 30, 2019) and measurement data

No.	Coordinate (m)		Land surface temperature (°C)	Measurement value (°C)	Difference (°C)
	X	Y			
1	586736	2358680	36.2	35.0	1.2
2	586885	2358780	44.9	42.2	2.7
3	587154	2358840	46.9	44.0	2.9
4	586604	2359260	47.7	44.6	3.1
5	586157	2359350	46.3	43.9	2.4
6	586416	2359790	43.9	41.3	2.8
7	586240	2359600	44.9	42.6	2.3
8	586546	2359510	46.7	43.8	2.9
9	586355	2359040	43.6	41.5	2.1
10	586207	2359200	47.6	45.0	2.6



Figure 8. Some pictures in the Nam Son landfill taken during the September 30, 2019 survey: incinerators (a), garbage dump (b, c), wastewater treatment facilities (d)

## 4. Conclusion

Land surface temperature is one of the most important factors in environmental studies, including environmental pollution problem in the surrounding area of landfills. Remote sensing technology with advantages such as wide area coverage and short revisit interval has been used effectively in determining the landfills surface temperature, thereby providing the input information of model to estimate landfill pollution.

Analysis of the results obtained from the two test areas (Nam Son and Da Phuoc landfills) shows that, the landfill surface temperature is often higher than 40°C and is much higher than the surrounding area temperature. The difference between the highest land surface temperature (at the landfill) and the lowest land surface temperature (at the area covered by vegetation) in both test areas was about 20 degrees. The results obtained in the study provide timely information to help managers take measures to cope with environmental pollution around landfills.

## References

1. Boori M.S., Vozenilek V., Balter H., Choudhary K. (2015). Land surface temperature with land cover classes in Aster and Landsat data. *Journal of Remote Sensing & GIS*, 4:138, 1-4, doi:10.4172/2169-0049.1000138.
2. Bui Q.T. (2015). Urban heat island analysis in Ha Noi: examining the relationship between land surface temperature and impervious surface, *Conference of Application of GIS 2015*, 674-677.
3. Chavez P. (1996). Image-based atmospheric corrections-revisited and improved. *Photogrammetric Engineering and Remote Sensing*, 62(9), 1025-1036.
4. Chen F., Yang S., Su Z., Baoyin H. (2015). A new single-channel method for estimating land surface temperature based on the image inherent information: the HJ-1B case, *ISPRS Journal of Photogrammetry and Remote Sensing*, 101, 80-88.
5. Dancheva A., Spasova T., Borisova D. (2019). Evaluation of temperature changes in waste disposal sites according to satellite data. Proc. *SPIE 11174, 17<sup>th</sup> International Conference on Remote Sensing and Geoinformation of the Environment (RSCy2019)*, 11174Q, <https://doi.org/10.1117/12.2533609>.
6. Du C., Ren H., Qin Q., Meng J., Li J. (2014). Split-window algorithm for estimating land surface temperature from Landsat 8 TIRS data, *International Geosciences Remote Sensing Symposium*, 3578-3581, <https://doi.org/10.1109/IGARSS.2014.6947256>.
7. Galve J.M., Coll C., Caselles V., Valor E., Mira M. (2008). Comparison of split-window and single-channel methods for land surface temperature retrieval from MODIS and ASTER data. *International Geoscience Remote Sensing Symposium*, 3, 294-297, <https://doi.org/10.1109/IGARSS.2008.4779341>.

8. Gill J., Faisal K., Shaker A., Yan W. (2019). Detection of waste dumping locations in landfill using multi-temporal Landsat thermal images. *Waste Management and Research*, 37(4), 386-393, doi: 10.1177/0734242X18821808.
9. Guha S., Govil H., Dey A., Gill N. (2018). Analytical study of land surface temperature with NDVI and NDBI using Landsat 8 OLI and TIRS data in Florence and Naples city, Italy. *European Journal of Remote Sensing*, 51(1), 667-678, <https://doi.org/10.1080/22797254.2018.1474494>.
10. Huazhong R., Du C., Qin Q., Liu R. (2014). Atmospheric water vapor retrieval from Landsat 8 and its validation. *IEEE International Geoscience and Remote Sensing Symposium*, 3045-3048, doi: 10.1109/IGARSS.2014.6947119.
11. Jiménez-Muñoz J.C, Sobrino J.A., Skoković D., Mattar C., Cristóbal J. (2014). LST retrieval methods from Landsat-8 thermal infrared sensor data. *IEEE Geoscience and Remote Sensing Letters*, 11(10), 1840-1843, doi: 10.1109/LGRS.2014.2312032.
12. Li S., Jiang G. (2018). Land surface temperature retrieval from Landsat-8 data with the generalized split-window algorithm. *IEEE Access*, 6, 18149-18162, doi:10.1109/ACCESS.2018.2818741.
13. Pal S., Ziaul S. (2017). Detection of land use and land cover change and land surface temperature in English Bazar urban centre. *The Egyptian Journal of Remote Sensing and Space Science*, 20(1), 125-145.
14. Qdais H.A., Shatnawi N. (2019). Assessing and predicting landfill surface temperature using remote sensing and an artificial neural network. *International Journal of Remote Sensing*, 40(24), 9556-9571.
15. Rongali G., Keshari A.K., Gosain A.K., Khosa R. (2018). Split-window algorithm for retrieval of land surface temperature using Landsat 8 thermal infrared data. *Journal of Geovisualization and Spatial Analysis*, 2(2), 1-19.
16. Rouse J.W., Hass R.H., Schell J.A., Deering D.W. (1973). Monitoring vegetation systems in the Great Plains with ERTS. In: *Earth Resources Technology Satellite-1 Symposium*, 3, Washington- DC, 309-317.
17. Rozenstein O., Qin Z., Derimian Y., Karnieli A. (2014). Derivation of land surface temperature for Landsat-8 TIRS using a split window algorithm. *Sensors*, 14, 5768-5780, <https://doi.org/10.3390/s140405768>.
18. Sobrino J.A., Jimenez-Munoz J.C., Zarco-Tejada P.J., Guadalupe Sepulcre-Canto, Eduardo de Miguel (2006). Land surface temperature derived from airborne hyperspectral scanner thermal infrared data. *Remote Sensing of Environment*, 102, 99-115.
19. Tran T.V., Hoang T.L., Le V.T. (2009). Thermal remote sensing method in study on urban surface temperature distribution. *Vietnam Journal of Earth Sciences*, 31(2), 168-177.

20. Trinh L.H. (2018). Combined use of Landsat 8 and Sentinel 2 images for enhanced spatial resolution of land surface temperature. *VNU Journal of Science: Earth and Environmental Sciences*, 34(4), 54-63.
21. Trinh L.H., Vu D.T. (2019). Comparison of single-channel and split-window methods for estimating land surface temperature from Landsat 8 data. *VNU Journal of Science: Earth and Environmental Sciences*, 35(2), 33-44.
22. Yu X., Guo X., Wu X. (2014). Land surface temperature retrieval from Landsat 8 TIRS – Comparison between radiative transfer equation based method, split window algorithm and single channel method. *Remote Sensing*, 6, 9829-9852, doi:10.3390/rs6109829.
23. Valor E., Caselles V. (1996). Mapping land surface emissivity from NDVI. Application to European African and South American areas. *Remote Sensing of Environment*, 57, 167-184.
24. Vlassova L., Perez-Cabello F., Nieto H., Martin P., Riaflo D., de la Riva J. (2014). Assessment of methods for land surface temperature retrieval from Landsat 5 TM images applicable to multiscale tree-grass ecosystem modeling. *Remote Sensing*, 6, 4345-4368; doi:10.3390/rs6054345.
25. United State Geological Survey (USGS). *Landsat 8 data users handbook*, Available at website <http://usgs.gov>, January 12, 2020.
26. <https://earthexplorer.usgs.gov/>, Accessed December 15, 2019.

## ĐÁNH GIÁ PHÂN BỐ NHIỆT ĐỘ BỀ MẶT CÁC BÃI RÁC THẢI TẠI CÁC THÀNH PHỐ LỚN Ở VIỆT NAM TỪ ẢNH VỆ TINH LANDSAT 8

**Tóm tắt:** Trong những năm qua, quá trình đô thị hóa và gia tăng dân số nhanh chóng dẫn đến tình trạng quá tải rác thải ở các thành phố lớn. Nhiệt độ bề mặt cao ở các bãi rác thải cũng là một nhân tố gây nên tình trạng ô nhiễm môi trường nghiêm trọng. Bài báo này trình bày kết quả đánh giá phân bố nhiệt độ bề mặt ở một số bãi rác thải lớn ở Việt Nam, bao gồm bãi rác thải Nam Sơn (Hà Nội) và Đa Phước (Thành phố Hồ Chí Minh). Dữ liệu ảnh vệ tinh Landsat 8 được sử dụng để tính toán nhiệt độ bề mặt trên cơ sở phương pháp split-window. Kết quả nhận được cho thấy, nhiệt độ bề mặt các bãi rác thải cao hơn rất nhiều so với khu vực xung quanh, thậm chí so với các khu vực được đặc trưng bởi các mặt không thấm. Chênh lệch giữa nhiệt độ cao nhất tại bãi rác Nam Sơn, Đa Phước và nhiệt độ thấp nhất ở khu vực xung quanh đạt khoảng 20°C. Kết quả nhận được trong nghiên cứu cung cấp thông số đầu vào trong xây dựng các mô hình giám sát ô nhiễm môi trường tại các bãi rác thải.

**Từ khóa:** Bãi rác thải; nhiệt độ bề mặt; viễn thám; hồng ngoại nhiệt; Landsat 8.

*Received: 31/3/2020; Revised: 21/8/2020; Accepted for publication: 23/12/2020*

